IET Generation, Transmission & Distribution

Research Article

Decentralised hybrid robust/stochastic expansion planning in coordinated transmission and active distribution networks for hosting large-scale wind energy

ISSN 1751-8687
Received on 9th June 2019
Revised 31st August 2019
Accepted on 25th September 2019
E-First on 13th January 2020
doi: 10.1049/iet-gtd.2019.0888
www.ietdl.org

Ahmad Nikoobakht[1], Jamshid Aghaei[2,3] ✉, Hamid Reza Massrur[4], Rasul Hemmati[5]

[1]*Higher Education Center of Eghlid, Eghlid, Iran*
[2]*Department of Electrical and Electronics Engineering, Shiraz University of Technology, Shiraz, Iran*
[3]*Department of Electric Power Engineering, Norwegian University of Science and Technology (NTNU), Trondheim NO-7491, Norway*
[4]*The Centre of Excellence in Power System Control and Management, Electrical Engineering Department, Sharif University of Technology, Tehran, Iran*
[5]*Department of Electrical Engineering, Marquette University, USA*
✉ *E-mail: jamshid.aghaei@ntnu.no*

Abstract: Today, coordinated expansion planning is one of the key challenges for electricity systems including active distribution networks (ADNs) and transmission networks (TNs) hosting distributed renewable generation as well as large-scale wind energy generation. Accordingly, this study presents a decentralised hybrid robust and stochastic (HR&S) expansion planning optimisation method to determine a robust generation and transmission planning for a TN and stochastic expansion planning for ADNs. The proposed HR&S planning model is formulated with the objective of achieving an effective expansion of both TN&ADN while minimises the investment and operation costs of TN&ADN planning considering wind uncertainty in TNs and load uncertainty in ADNs. Finally, the IEEE 30-bus test system has been analysed to show the effectiveness of the proposed TN&ADN expansion planning framework and decentralised solution strategy.

Nomenclature

A. Indices

y	index of planning years
t	index of time blocks
w, g	index for generating units and wind farms, respectively
k/l	index of transmission lines/feeders
n, m	index of TN buses
i, j	index of ADN buses
ℓ/ι	index of linearisation segments of voltage angle term/ circular constraint.
$(\bullet)_{s,(\cdot)}$	related to scenario s
$(\bullet)_{(\cdot),t}$	related to element $(\cdot)$ at time period t

Parameters

$C_g^{\mathrm{TOP}}/C_{n,i}^{\mathrm{DOP}}$	operation cost of the generator/distribution unit
$C_g^{\mathrm{TIG}}/C_k^{\mathrm{TIL}}$	investment cost of the generator unit/ transmission line
$C_{n,i}^{\mathrm{DIG}}/C_{n,l}^{\mathrm{DIL}}$	investment cost of distribution generator unit/ feeder
$\bar{\Theta}^{\mathrm{TIG}}/\bar{\Theta}^{\mathrm{TIL}}$	investment budget for a new generating units/ transmission lines
$\bar{\Theta}^{\mathrm{DIG}}/\bar{\Theta}^{\mathrm{DIL}}$	investment budget for new distributed generations (DGs)/feeders
ρ_s	probability of scenario s
$C_{n,i}^{\mathrm{CPE}}$	cost of power exchange between TN&AND
$\mathrm{PG}_{(\cdot)}^{\min}/\mathrm{PG}_{(\cdot)}^{\max}$	min/max active power generation
$\mathrm{QG}_{(\cdot)}^{\min}/\mathrm{QG}_{(\cdot)}^{\max}$	min/max reactive power generation
$\mathrm{PD}_{(\cdot)}/\mathrm{QD}_{(\cdot)}$	active/reactive load demand
$g_{(\cdot)}/b_{(\cdot)}$	conductance/admittance of a line (or feeder)
$\mathrm{Sl}_{(\cdot)}^{\max}/\mathrm{Pl}_{(\cdot)}^{\max}$	maximum value of the MVA/MW power flow through a line (or feeder)
$\eta_{(\cdot)}$	power factor on a bus
$\bar{P}_{(\cdot)}^{w}$	forecasted wind power
Γ_w	budget of uncertainty
$V_{(\cdot)}^{\max}/V_{(\cdot)}^{\min}$	max/min voltage magnitude
$\varphi_{(\cdot)}^{\max}/\varphi_{(\cdot)}^{\min}$	max/min voltage angle difference across a line (or feeder)
$\bar{\varphi}_{\ell}$	length of each piecewise linear segment, in radians
$\gamma_{(\cdot),\ell,nm}, \lambda_{(\cdot),\ell,nm}$	constants in the ℓth linear segment
$\boldsymbol{I}'/\boldsymbol{C}', \tilde{\boldsymbol{I}}'/\tilde{\boldsymbol{C}}'$	coefficient matrices for investment/operation cost in TN and ADN planning
α/β	multipliers of the penalty function
M	large enough constant
π_t	number of hours in time block t
$\sigma^{\mathrm{T}}/\sigma^{\mathrm{D}}$	weighting factor in TN/ADN to make comparable operation costs and investment
r	discount rate.

Variables

Φ^{TN}	total cost of TN planning
Φ_n^{ADN}	total cost of ADN planning
$\mathrm{PG}_{(\cdot)}/\mathrm{QG}_{(\cdot)}$	active/reactive power generation.
$\mathrm{Pl}_{(\cdot)}/\mathrm{Ql}_{(\cdot)}$	active/reactive power flow.
$\tilde{\mathrm{Pl}}_{(\cdot)}/\tilde{\mathrm{Ql}}_{(\cdot)}$	active/ reactive power flow.
$\psi_{(\cdot),nm}$	piecewise linearisation of $\cos(\varphi_{(\cdot),nm})$.
$\vartheta_{(\cdot),\ell,nm}$	status of the ℓth linear segment of line (n, m).
$P_{y,t}^{w}$	wind power generation.
$\mathrm{PS}_{(\cdot)}/\mathrm{QS}_{(\cdot)}$	active/reactive power provided by a substation in AND.
$z^{\mathrm{T}}/z^{\mathrm{D}}$	vector of target/response variable
u^{T}	polyhedral uncertainty sets
$\upsilon_{(\cdot),g}$	binary variable for the state of generating units
$x_{y,g}^{\mathrm{G}}/x_{y,k}^{\mathrm{TL}}$	binary variable that equals 1 if the gth/kth (generator unit)/ (transmission line) in TN planning is built, and 0 otherwise

$x^{\mathrm{DG}}_{y,n,i}/x^{\mathrm{DL}}_{y,n,l}$	binary variable that equals 1 if the *g*th/*k*th (DG)/(feeder) in ADN planning is built, and 0 otherwise
$\varphi_{y,t,(\cdot)}$	voltage angle difference across a line
$V_{y,t,(\cdot)}$	voltage-magnitude
$\kappa^{\mathrm{T}}_{(\cdot)}$	dual variables associated with the corresponding constraints
x^{Ω}/y^{Ω}	investment/operation decision variables.
θ	value of operation cost

Sets

Ω_g/Ω_g^+	existing/prospective generating units
Ω_k/Ω_k^+	existing/prospective transmission lines
Ω_i/Ω_i^+	existing/prospective DGs
Ω_l/Ω_l^+	existing/prospective feeders

1 Introduction

In recent years, growth of load demand and renewable generation capacity, especially wind energy generation (WEG) with variable and unpredictable nature, pose two main challenges to serve electricity demand in a power system for the coming years with acceptable reliability:

(i) The scarcity of transmission capacity and transmission congestion in a transmission network (TN) are made resulting in preventing the absorption of WEG and optimal commitment of cheaper generating units (GUs).
(ii) The limited predictability and controllability of WEG are expected to need large volumes of flexible generation capacity which involves adverse economic effects.

In order to address the first challenge, building additional transmission lines (TLs) is a feasible solution. However, transmission expansion planning (TEP) as a regular solution is a costly choice for mitigating these bottlenecks, especially with WEG integration. The TEP is to determine where and when to construct new TLs with the aim of providing sufficient transmission capacity to serve the increasing load demand and deliver high penetration of WEG to loads [1]. Although the TEP approach can solve the first challenge, it fails to provide sufficient flexible generation capacity to cover the uncertainty of the variable output of wind farms. Accordingly, in this study, the generation expansion planning (GEP) is introduced in order to address the second challenge [2]. The GEP is considered one of the major parts of TN planning that could solve the deficiency of flexible generation capacity in power system operation. Although this approach is interesting, it is often very costly in the TN expansion planning scheme [2]. Under this circumstance, this study finds another option to relieve transmission bottlenecks, enhance generation capacity and reduce the cost of TN expansion planning through the utilisation of active distribution networks (ADNs). Owing to the integration of distributed generations (DGs), the distribution network is changed from passive status to an ADN, in other words, the ADN can be utilised as a controllable demand in transmission buses [3]. Accordingly, expansion planning of ADN can play a critical role in providing demand side flexibility in TN planning. The expansion planning of ADNs seeks to define the capacity of the DGs and feeders where and when they should be installed to meet forecasted demand with acceptable quality standards and minimal cost.

A point often overlooked, the coordinated planning between transmission and active distribution systems could help to postpone the upgrading of the TN&ADNs, reduce the investment cost and improve the asset utilisation, which improves the social welfare and performance of the whole power system. Undoubtedly, with the coordination of TN&ADN expansion planning, coordinated TN planning may save some unnecessary investment in ADNs, which can be impossible to handle using only ADN planning due to incomplete construction conditions. Likewise, some weaknesses in a TN planning could also be removed by the coordinated ADNs planning. However, this point must be remembered that in almost all TEP and GEP (T&GEP) in TN expansion planning problems, the ADNs are only treated as load injections into the transmission buses (these connection buses are called 'boundary buses'), and DG units output and inner optimal power flow (PFs) of the ADNs are not measured [4, 5]. This assumption may reduce the running time of the TN expansion planning problem but neglects the role of ADNs in providing flexibility in transmission system planning [6].

On the other hand, currently, solving the T&GEP problem with an entire transmission and distribution network model in a centralised framework faces some challenges such as (i) once considering both the TN&ADNs in planning problem, a large number of non-linear PF equations with continuous/discrete variables make difficulties in finding a solution for the centralised framework; (ii) excessive differences in, line parameter values, power levels, and voltage levels of the TN&ADNs lead to numerical problems; and (iii) in real world, the TN&ADNs are separately operated, hence, co-operation of both TN&ADNs in a centralised framework is against privacy protection rules, and it is ineligible to directly solve a whole TN&ADNs model in the centralised framework. According to the above-mentioned challenges, the PF is an important tool to describe the interactions of transmission and distribution systems [7, 8]. Typically, most studies in the field of the T&GEP problem in TN have only focused on DC PF equations [1, 2, 9]. Nonetheless, the assumptions of DC PF equations are not credible in distribution systems since the resistance to reactance ratio (R/X) of distribution lines is high. As a result, the AC PF is the only proper approach that can be used in the distribution systems [8, 10]. On the other hand, in order to obtain optimal results for the planning problem, a similar PF tool should be applied for both TN&ADNs planning. However, current commercial mixed integer non-linear programming (MINLP) solvers are not able to find the global optimal solution for the planning problems with AC PF equations mixed with binary variables because they are mixed integer non-linear problems [11]. Hence, in order to overcome the above-mentioned challenge, a linear AC PF model is proposed for the planning and operation in TN&ADNs. In fact, the linear AC PF model converts this MINLP problem into a mixed integer linear programming (MILP), thus, this problem has a globally optimal solution that could be solved with available MILP solvers [11].

Another key point is that it is very challenging to handle the wind and load uncertainties in the TN&ADNs expansion planning. Either overrating or underestimating the effect of wind and load uncertainties in planning decisions could possibly increase investment costs and threaten the power-supply reliability.

In order to develop an advanced uncertainty management scheme, it is necessary to classify the uncertainties for the expansion planning problem. Thus, here, uncertainties can be classified as follows:

- Non-haphazard uncertainties happen in lower frequency and larger time scale, which are simple to accurately fit into any probability density functions (PDFs) because of data sufficiency. The load uncertainty falls into this class.
- Haphazard uncertainties repeatable in a high-frequency and short period, which is difficult to accurately fit into any distribution due to data insufficiency. The wind uncertainty is a typical sample in this class.

Stochastic optimisation method (SOM) is a common tool to handle the non-haphazard uncertainties in TN&ADN planning. The key idea of the SOM is to employ a limited set of scenarios to denote the possible realisations of non-haphazard uncertainties [12, 13]. The main disadvantage of the SOM is that this method is less appropriate once data is inaccurate or unavailable. The TN&ADN planning under haphazard uncertainties, whose PDFs are unknown, is studied using the uncertainty set approach, e.g. robust optimisation method (ROM). This method only needs uncertainty sets rather than PDFs to represent the haphazard uncertainties and make planning decisions under the worst scenarios within those sets. Nevertheless, this method is not appropriate for non-haphazard uncertainties due to its over conservatism, it makes planning decision under the worst scenario because the worst scenario occurs frequently in haphazard uncertainty, not non-haphazard uncertainty. Accordingly, the investment and operation costs in the TN&ADN planning scheme mostly depend on the type of uncertainty and a hybrid optimisation method is needed to concurrently handle non-haphazard and haphazard uncertainties. Therefore, a hybrid robust and stochastic (HR&S) optimisation method has been proposed in this study.

A considerable amount of literature has focused on expansion planning in TN or ADNs based on SOM or ROM. An expansion model of T&GEP in a TN using ROM has been proposed in [1] wherein the uncertainties have been represented by uncertainty sets. In [14], the planning of transmission systems in TN has been proposed based on a stochastic model. A two-stage stochastic planning model is used in [15] to solve the T&GEP problem considering wind power and system load uncertainties. Besides, in [16, 17], a stochastic planning model is proposed to install feeders and distributed generation (DGs) in the ADN. A multi-stage expansion planning in ADN based on piecewisely linearised AC PF is proposed in [18], in order to obtain the optimal planning of DGs, configuration, feeder and substation capacities. In this work, uncertainty has been modelled by dissimilar scenarios of WEG and load demand according to a PDF.

The model proposed in this study differs from the above references in two aspects: (i) in comparison with [1, 14–18], the impact of the coordination between TN&ADNs on the planning scheme has not been investigated. (ii) Although the SOM or ROM is independently used for planning models in [1, 14–18], while the model proposed in this study is developed based on the HR&S optimisation method. Accordingly, coordination between TN&ADNs based on the HR&S planning scheme is nowadays needed to fully exploit their advantages.

According to the above-mentioned challenges, after addressing PF and uncertainty model challenges, there is still another challenge about how to solve the HR&S planning problem for centralised TN&ADNs?

In response to the above question, an iterative decomposition solution approach based on a decentralised optimisation algorithm and primal Benders' decomposition algorithm has been proposed in this study to solve the HR&S planning problem for the coordinated TN&ADNs. A major advantage of this solution strategy is that the expansion planning for TN&ADNs can be calculated by iteratively running transmission and distribution PF programmes that are connected in different control centres, and only the active, reactive powers and voltages of the boundary buses are communicated between the control centres. Furthermore, under certain sufficient conditions, a linear convergence of the proposed solution strategy with high accurate results can be mathematically guaranteed.

Briefly, the contributions of this study include

(i) Developing a hybrid stochastic and robust method to solve an integrated TN&ADNs hosting large-scale WEG under the wind and load uncertainties; the proposed method takes the advantages of both stochastic and robust optimisation methods. It can provide an expansion planning decision with minimum investment and operation costs while ensuring the system's robustness.
(ii) An iterative decomposition optimisation algorithm based on the decentralised optimisation algorithm and primal Benders' decomposition algorithm has been presented to solve the HR&S planning scheme for TN&ADNs.

2 Centralised co-planning of TN&ADNs

2.1 Assumptions

For the sake of transparency, the key assumptions of the proposed model are summarised as follows:

- Only wind uncertainty (haphazard uncertainty) in TN planning has been considered because this research study focuses on hosting large-scale WEG. Nevertheless, the proposed model is capable of considering load uncertainty as well.
- In ADNs planning only load uncertainty (non-haphazard uncertainty) has been considered. However, the proposed ADNs planning model is capable of considering the uncertainty of DG output as well.
- The ROM is used to model the wind uncertainty, by using uncertainty sets, in the TN planning scheme. Similarly, in the ADNs planning scheme, the SOM has been used to model the load uncertainty by using a set of scenarios.

The detailed formulation of the centralised HR&S co-planning of T&GEP in TN&ADNs is provided as follows.

2.2 Objective function

$$\Phi^{\mathrm{TC}} = \min_{\Xi_1} \max_{\Xi_2} \min_{\Xi_3} \Phi^{\mathrm{TN}} + \min_{\Xi_4^n} \sum_{n \in \Omega_n^{\mathrm{ADN}}} \Phi_n^{\mathrm{ADN}} \tag{1}$$

where $\Xi_1 = \left\{x_{y,g}^{\mathrm{G}}, x_{y,k}^{\mathrm{TL}}, x_{y,n,i}^{\mathrm{DG}}, x_{y,n,l}^{\mathrm{DL}}\right\}$, $\Xi_2 = \left\{P_{y,t}^{w}\right\}$, $\Xi_3 = \left\{\mathrm{PG}_{y,t,g}, \mathrm{QG}_{y,t,g}, \mathrm{Pl}_{y,t,nm}, \mathrm{Ql}_{y,t,nm}, V_{y,t,n}, \varphi_{y,t,nm}, \tilde{\mathrm{Pl}}_{y,t,nm}, \tilde{\mathrm{Ql}}_{y,t,nm}, P_{y,t,n}, Q_{y,t,n}\right\}$
and

$$\Xi_4^n = \left\{\begin{matrix} \mathrm{PG}_{s,y,t,i}, \mathrm{QG}_{s,y,t,i}, \varphi_{s,y,t,ij}, \mathrm{Pl}_{s,y,t,ij}, \mathrm{Ql}_{s,y,t,ij} \\ \tilde{\mathrm{Pl}}_{s,y,t,ij}, \tilde{\mathrm{Ql}}_{s,y,t,ij}, V_{s,y,t,i}, \mathrm{PS}_{\mathrm{y,t,i}}, \mathrm{QS}_{y,t,i} \end{matrix}\right\}.$$

The objective function (1) represents the min–max–min consecutive structure of a robust optimisation model for the TN planning and a minimisation structure of a stochastic optimisation model for ADNs planning. Indeed, the objective function (1) denotes the total cost (TC) for the TN&ADNs planning scheme, which includes the TN plus ADNs planning costs. More details about the constraints for the TN&ADNs planning are given in the following section.

2.3 Robust TN planning constraints

$$\begin{aligned}\Phi^{\mathrm{TN}} = & \sum_{y} \sum_{g \in \Omega_g^+} \frac{C_g^{\mathrm{TIG}}\left(x_{y,g}^{\mathrm{G}} - x_{y-1,g}^{\mathrm{G}}\right)}{(1+r)^{y-1}} \\ & + \sum_{y} \sum_{k \in \Omega_k^+} \frac{C_g^{\mathrm{TIL}}\left(x_{y,k}^{\mathrm{TL}} - x_{y-1,k}^{\mathrm{TL}}\right)}{(1+r)^{y-1}} \\ & + \beta \sum_{y} \sum_{t} \pi_t \sum_{g} \frac{C_g^{\mathrm{TOP}} \mathrm{PG}_{y,t,g}}{(1+r)^{y-1}}\end{aligned} \tag{2}$$

$$x_{y,g}^{\mathrm{G}}, x_{y,k}^{\mathrm{TL}} \in \{0,1\}; \quad \forall g \in \Omega_g^+, k \in \Omega_k^+ \tag{3}$$

$$x_{y,g}^{\mathrm{G}}, x_{y,k}^{\mathrm{TL}} = 1; \quad \forall g \in \Omega_g/\Omega_g^+, k \in \Omega_k/\Omega_k^+ \tag{4}$$

$$x_{y,g}^{\mathrm{G}} \geq x_{y-1,g}^{\mathrm{G}} \tag{5}$$

$$x_{y,k}^{\mathrm{TL}} \geq x_{y-1,k}^{\mathrm{TL}} \tag{6}$$

$$\sum_{y} \sum_{g \in \Omega_g^+} \frac{C_g^{\mathrm{TIG}}\left(x_{y,g}^{\mathrm{G}} - x_{y-1,g}^{\mathrm{G}}\right)}{(1+r)^{y-1}} \leq \bar{\Theta}^{\mathrm{TIG}} \tag{7}$$

$$\sum_{y} \sum_{k \in \Omega_k^+} \frac{C_g^{\mathrm{TIL}}\left(x_{y,k}^{\mathrm{TL}} - x_{y-1,k}^{\mathrm{TL}}\right)}{(1+r)^{y-1}} \leq \bar{\Theta}^{\mathrm{TIL}} \tag{8}$$

$$0 \leq \mathrm{PG}_{y,t,g} \leq \mathrm{PG}_g^{\max} x_{y,g}^{\mathrm{G}} \tag{9}$$

$$0 \leq \mathrm{QG}_{y,t,g} \leq \mathrm{QG}_g^{\max} x_{y,g}^{\mathrm{G}} \tag{10}$$

$$\mathrm{Pl}_{y,t,nm} = g_k V_{y,t,n}^2 - V_{y,t,n} V_{y,t,m}\left(g_k \cos\varphi_{y,t,nm} + b_k \sin\varphi_{y,t,nm}\right) \tag{11}$$

$$\begin{aligned}\mathrm{Ql}_{y,t,nm} = & -(b_k + b_{k0}) V_{y,t,n}^2 - V_{y,t,n} V_{y,t,m} \\ & \left(b_k \cos\varphi_{y,t,nm} - g \sin\varphi_{y,t,nm}\right)\end{aligned} \tag{12}$$

$$\mathrm{Pl}_{y,t,nm} - M\left(1 - x_{y,k}^{\mathrm{TL}}\right) \le \tilde{\mathrm{P}}\mathrm{l}_{y,t,nm} \le \mathrm{Pl}_{y,t,nm} + M\left(1 - x_{y,k}^{\mathrm{TL}}\right) \quad (13)$$

$$\mathrm{Ql}_{y,t,nm} - M\left(1 - x_{y,k}^{\mathrm{TL}}\right) \le \tilde{\mathrm{Q}}\mathrm{l}_{y,t,nm} \le \mathrm{Ql}_{y,t,nm} + M\left(1 - x_{y,k}^{\mathrm{TL}}\right) \quad (14)$$

$$\tilde{\mathrm{P}}\mathrm{l}_{y,t,nm}^2 + \tilde{\mathrm{Q}}\mathrm{l}_{y,t,nm}^2 \le (\mathrm{Sl}_{nm}^{\max})^2 x_{y,k}^{\mathrm{TL}} \quad (15)$$

$$-\mathrm{Pl}_k^{\max} x_{y,k}^{\mathrm{TL}} \le \tilde{\mathrm{P}}\mathrm{l}_{y,t,nm} \le \mathrm{Pl}_k^{\max} x_{y,k}^{\mathrm{TL}} \quad (16)$$

$$-\mathrm{Sl}_k^{\max} x_{y,k}^{\mathrm{TL}} \le \tilde{\mathrm{Q}}\mathrm{l}_{y,t,nm} \le \mathrm{Sl}_k^{\max} x_{y,k}^{\mathrm{TL}} \quad (17)$$

$$V_n^{\min} \le V_{y,t,n} \le V_n^{\max} \quad (18)$$

$$\varphi_k^{\min} \le \varphi_{y,t,nm} \le \varphi_k^{\max} \quad (19)$$

$$\sum_{g(n)} \mathrm{PG}_{y,t,g} - \sum_{k(n,m)} \tilde{\mathrm{P}}\mathrm{l}_{y,t,nm} - \mathrm{PD}_{y,t,n} = -\sum_{w(n)} P_{y,t}^w \quad (20)$$

$$\sum_{g(n)} \mathrm{QG}_{y,t,g} - \sum_{k(n,m)} \tilde{\mathrm{Q}}\mathrm{l}_{y,t,nm} = \eta_n \mathrm{QD}_{y,t,n} = Q_{y,t,n} \quad (21)$$

$$\Omega_{\mathrm{US}}^w = \left\{ \begin{array}{c} P_{y,t}^w \in \left[0, \bar{P}_{y,t}^w\right], \\ \sum_y \sum_t \sum_w \left(\dfrac{\bar{P}_{y,t}^w - P_{y,t}^w}{\bar{P}_{y,t}^w} \right) \le \bar{\Gamma}_w \end{array} \right\} \quad (22)$$

The corresponding optimisation objective function of the TN in the planning problem is to minimise the investment (i.e. GU and TL construction) and operation (i.e. generation) costs, under the worst-case wind uncertainty realisation, which can be expressed by (2). Note that in (2), the investment decisions relating to transmission and generation construction are made before the worst-case uncertainty realisation. Actually, constraint (2) denotes the TC in the TN planning, including (i) investment cost (IC) of building new generation unit (first term) and installing new TLs (second term) and (ii) the operation cost (OC) of conventional generation units (third term). Note that the OCs are multiplied by parameter π_t which is the number of hours corresponding to time block t. Constraints (3) and (4) define the prospective and existing generation units and TLs, respectively. Constraints (5) and (6) indicate that when a new generation unit and a new line are constructed, they will exist during the rest of the planning horizon. Constraints (7) and (8) guarantee that the IC of GUs and TLs do not exceed their available investment budgets, respectively. Constraints (9) and (10) impose the active and reactive capacity limits of the generation units, respectively. Constraints (11) and (12) indicate non-linear active and reactive PF equations for each line, respectively. Constraints (13) and (14) show active and reactive PF in the prospective and existing TLs, respectively. Apparent PF, active and reactive PF limits for both the existing and prospective lines, respectively, are shown by (15), (16) and (17). Constraints (18) and (19) put a limit on the voltage magnitude at buses and the phase angle difference across lines, respectively. Constraints (20) and (21) show active and reactive power balance at each bus, respectively. In this study, the WEG uncertainties are modelled in terms of polyhedral uncertainty sets [1]. As WEG forecast value $\bar{P}_{y,t}^w$ could be inaccurate, $P_{y,t}^w$ is implemented to denote possible WEG realisations that could take any value within the uncertain intervals, i.e. $P_{y,t}^w \in \left[0, \bar{P}_{y,t}^w\right]$. In (22), constraint $\sum_y \sum_t \sum_w \left(\left(\bar{P}_{y,t}^w - P_{y,t}^w\right)/\bar{P}_{y,t}^w\right) \le \Gamma_w$ handles the total deviations of WEGs from their forecast values throughout the whole planning horizon, where Γ_w is a constant that can take values between 0 and $\Gamma_w^{\max}$, which is named the degree of robustness. If $\Gamma_w = 0$, then $\bar{P}_{y,t}^w = P_{y,t}^w$, i.e. the wind power generation uncertainty is not considered. However, if $\Gamma_w = \Gamma_w^{\max}$, then $P_{y,t}^w$ can take any value within the interval $\left[0, \bar{P}_{y,t}^w\right]$, which can be seen as the case of the maximum level of uncertainty.

2.4 Stochastic ADN planning constraints

The corresponding stochastic optimisation objective function of the ADN planning in the proposed problem is to minimise the IC and OC, which can be formulated by (23). Equation (23) includes the four terms as follows: the DGs and feeders building costs (first and second terms), expected operation cost of DGs (third term) and purchased energy from the substation or TN (fourth term)

$$\begin{aligned} \Phi_n^{\mathrm{ADN}} = & \sum_y \sum_{i \in \Omega_i^+} \frac{C_{n,i}^{\mathrm{DIG}}\left(x_{y,n,i}^{\mathrm{DG}} - x_{y-1,n,i}^{\mathrm{DG}}\right)}{(1+r)^{y-1}} \\ & + \sum_y \sum_{l \in \Omega_l^+} \frac{C_{n,l}^{\mathrm{DIL}}\left(x_{y,n,l}^{\mathrm{DL}} - x_{y-1,n,l}^{\mathrm{DL}}\right)}{(1+r)^{y-1}} \\ & + \beta \sum_s \rho_s \sum_y \sum_t \pi_t \sum_i \frac{C_{n,i}^{\mathrm{DOP}} \mathrm{PG}_{s,y,t,n,i}}{(1+r)^{y-1}} \\ & + \beta \sum_y \sum_t \pi_t \sum_i \frac{C_{n,i}^{\mathrm{CPE}} \mathrm{PS}_{y,t,n,i}}{(1+r)^{y-1}} \end{aligned} \quad (23)$$

$$x_{y,n,i}^{\mathrm{DG}}, x_{y,n,l}^{\mathrm{DL}} \in \{0, 1\}; \quad \forall i \in \Omega_i^+, l \in \Omega_l^+ \quad (24)$$

$$x_{y,n,i}^{\mathrm{DG}}, x_{y,n,l}^{\mathrm{DL}} = 1; \quad \forall i \in \Omega_i/\Omega_i^+, l \in \Omega_l/\Omega_l^+ \quad (25)$$

$$x_{y,n,i}^{\mathrm{DG}} \ge x_{y-1,n,i}^{\mathrm{DG}} \quad (26)$$

$$x_{y,n,l}^{\mathrm{DL}} \ge x_{y-1,n,l}^{\mathrm{DL}} \quad (27)$$

$$\sum_y \sum_{i \in \Omega_i^+} \frac{C_{n,i}^{\mathrm{DIG}}\left(x_{y,n,i}^{\mathrm{DG}} - x_{y-1,n,i}^{\mathrm{DG}}\right)}{(1+r)^{y-1}} \le \bar{\Theta}^{\mathrm{DIG}} \quad (28)$$

$$\sum_y \sum_{l \in \Omega_l^+} \frac{C_{n,l}^{\mathrm{DIL}}\left(x_{y,n,l}^{\mathrm{DL}} - x_{y-1,n,l}^{\mathrm{DL}}\right)}{(1+r)^{y-1}} \le \bar{\Theta}^{\mathrm{DIL}} \quad (29)$$

$$0 \le \mathrm{PG}_{s,y,t,i} \le \mathrm{PG}_i^{\max} x_{y,i}^{\mathrm{DG}} \quad (30)$$

$$0 \le \mathrm{QG}_{s,y,t,i} \le \mathrm{QG}_i^{\max} x_{y,i}^{\mathrm{G}} \quad (31)$$

$$\mathrm{Pl}_{s,y,t,ij} = g_k V_{s,y,t,i}^2 - V_{s,y,t,i} V_{s,y,t,j}\left(g_k \cos \varphi_{s,y,t,ij} + b_k \sin \varphi_{s,y,t,ij}\right) \quad (32)$$

$$\begin{aligned} \mathrm{Ql}_{s,y,t,ij} = & -(b_k + b_{k0}) V_{s,y,t,i}^2 - V_{s,y,t,i} V_{s,y,t,j} \\ & \left(b_k \cos \varphi_{s,y,t,ij} - g \sin \varphi_{s,y,t,ij}\right) \end{aligned} \quad (33)$$

$$\mathrm{Pl}_{s,y,t,ij} - M\left(1 - x_{y,l}^{\mathrm{TL}}\right) \le \tilde{\mathrm{P}}\mathrm{l}_{s,y,t,ij} \le \mathrm{Pl}_{s,y,t,ij} + M\left(1 - x_{y,l}^{\mathrm{TL}}\right) \quad (34)$$

$$\mathrm{Ql}_{s,y,t,ij} - M\left(1 - x_{y,l}^{\mathrm{TL}}\right) \le \tilde{\mathrm{Q}}\mathrm{l}_{s,y,t,ij} \le \mathrm{Ql}_{s,y,t,ij} + M\left(1 - x_{y,l}^{\mathrm{TL}}\right) \quad (35)$$

$$\tilde{\mathrm{P}}\mathrm{l}_{s,y,t,ij}^2 + \tilde{\mathrm{Q}}\mathrm{l}_{s,y,t,ij}^2 \le \left(\mathrm{Sl}_{ij}^{\max}\right)^2 x_{y,l}^{\mathrm{DL}} \quad (36)$$

$$\mathrm{Pl}_l^{\max} x_{y,l}^{\mathrm{DL}} \le \mathrm{Pl}_{s,y,t,ij} \le \mathrm{Pl}_l^{\max} x_{y,l}^{\mathrm{DL}} \quad (37)$$

$$\mathrm{Sl}_l^{\max} x_{y,l}^{\mathrm{DL}} \le \mathrm{Ql}_{s,y,t,ij} \le \mathrm{Sl}_l^{\max} x_{y,l}^{\mathrm{DL}} \quad (38)$$

$$V_i^{\min} \le V_{s,y,t,i} \le V_i^{\max} \quad (39)$$

$$\varphi_l^{\min} \le \varphi_{s,y,t,ij} \le \varphi_l^{\max} \quad (40)$$

$$\sum_i \mathrm{PG}_{s,y,t,i} + \sum_{i(n)} \mathrm{PS}_{y,t,i} - \sum_{l(i,j)} \tilde{P}_{s,y,t,ij} = \mathrm{PD}_{s,y,t,i} \quad (41)$$

$$\sum_i \mathrm{QG}_{s,y,t,i} + \sum_{i(n)} \mathrm{QS}_{y,t,i} - \sum_{l(i,j)} \tilde{\mathrm{Q}}\mathrm{l}_{s,y,t,ij} = \mathrm{QD}_{s,y,t,i} \quad (42)$$

$$\sum_l x_{y,l}^{\mathrm{DL}} = i - 1 \quad (43)$$

Constraints (24)–(42) are similar to constraints (3)–(21), respectively. To prevent any loop in the ADN and for maintaining the radial configuration in ADN planning scheme, constraint (43) is used [19].

2.5 Coupled constraints

$$\left.\begin{cases}\overbrace{\mathrm{PS}_{y,t,i}}^{\mathrm{ADN}} = \overbrace{\mathrm{PD}_{y,t,n}}^{\mathrm{TN}}\\ \mathrm{QS}_{y,t,i} = \mathrm{QD}_{y,t,n}\\ V_{s,y,t,i} = V_{y,t,n}\end{cases}\right\}\forall i \in i(n) \& n \in \Omega_n^{\mathrm{ADN}} \tag{44}$$

Here, constraint (44) links the TN and ADNs planning problems together. Thus, the constraint (44) includes active power, reactive power, and voltage equalities, respectively.

In constraint (44), $\mathrm{PD}_{y,t,n}$ and $\mathrm{QD}_{y,t,n}$ are the active and reactive loads in the TN. While $\mathrm{PS}_{y,t,i}$ and $\mathrm{QS}_{y,t,i}$ are the active and reactive power generations at substation bus for the ADN. Similarly, $V_{s,y,t,i}$ and $V_{y,t,n}$ are the voltage magnitudes at the ADN and TN sides, respectively. Note that the voltage magnitudes for all scenarios at the substation bus of ADN are equal.

2.6 Linearised AC PF

Here, a piecewise linearisation approach is used for linearised AC PF equations [11, 20]. At first, the following assumptions are considered in the linearisation procedure: (i) the voltage magnitude $V_{(\cdot)}$ is near to 1, for both TN and ADN, i.e. $0.95 \le V_{(\cdot)} \le 1.05$; (ii) the angle difference across a line (between two buses), for both TN and ADN, is very small, i.e. $|\varphi_{(\cdot)}| \le 10^{\circ}$. According to the second assumption, it is assumed $\sin(\varphi_{(\cdot)}) \simeq \varphi_{(\cdot)}$ and $\cos(\varphi_{(\cdot)}) \simeq 1$ [21, 22].Therefore, the active and reactive PFs (11), (12), (32), and (33) can be linearised as follows:

$$P_{(\cdot),nm} = g_k(V_{(\cdot),n} - V_{(\cdot),m} - \psi_{(\cdot),nm} + 1) - b_k(\varphi_{(\cdot),nm}) \tag{45}$$

$$Q_{(\cdot),nm} = -b_k(V_{(\cdot),n} - V_{(\cdot),m} - \psi_{(\cdot),nm} + 1) - g_k(\varphi_{(\cdot),nm}) \tag{46}$$

According to the second assumption, the piecewise linearisation of $\psi_{(\cdot),nm} = \cos(\varphi_{(\cdot),nm})$ in (45) and (46) can be obtained as follows:

$$\begin{cases}\psi_{(\cdot),nm} \le \gamma_{(\cdot),\ell,nm}\varphi_{(\cdot),nm} + \lambda_{(\cdot),\ell,nm} + M(1 - \vartheta_{(\cdot),\ell,nm})\\ \psi_{(\cdot),nm} \ge \gamma_{(\cdot),\ell,nm}\varphi_{(\cdot),nm} + \lambda_{(\cdot),\ell,nm} - M(1 - \vartheta_{(\cdot),\ell,nm})\end{cases} \tag{47}$$

$$\bar{\varphi}_{\ell}\vartheta_{(\cdot),\ell,nm} \le \varphi_{(\cdot),nm} \le \bar{\varphi}_{\ell+1}\vartheta_{(\cdot),\ell,nm} \tag{48}$$

$$\sum_{\ell} \vartheta_{(\cdot),\ell,nm} = 1 \tag{49}$$

At first, the angle difference across the line (*n, m*), i.e. $\varphi_{(\cdot),nm}$, is divided into L equal segment then the value of $\psi_{(\cdot),nm}$ for the ℓth segment can be calculated by constraint (47). Constraint (48) ensures that $\varphi_{(\cdot),nm}$ is placed on which segment, which is enforced using binary variable $\vartheta_{(\cdot),\ell,nm}$. Note that $\varphi_{(\cdot),nm}$ only can be placed on one segment, which is enforced by (49). Similarly, the non-linear equations of (15) and (36) are transformed into N linear equations as follows:

$$\begin{aligned}&\left(\sin\left(\frac{2\pi l}{N}\right) - \sin\left(\frac{2\pi(l-1)}{N}\right)\right)P_{(\cdot),nm}\\ &\left(\cos\left(\frac{2\pi l}{N}\right) - \cos\left(\frac{2\pi(l-1)}{N}\right)\right)Q_{(\cdot),nm}\\ &-\left|S_{nm}^{\max}\right|\sin\left(\frac{2\pi}{N}\right) \le 0\end{aligned} \tag{50}$$

Linear constraints (50) hold for $l = 1, 2,\ldots, N$. The higher the number of sides (*N*), the more precise the solution is, but at the expense of more computational burden. More details about piecewise linearisation can be found in [23].

3 Decentralised solution strategy

In order to solve the proposed HR&S planning problem for centralised TN&ADNs, the iterative decomposition algorithm is used. In fact, the iterative decomposition algorithm includes two main solution methods as follows: (i) the two-level hierarchical method and (ii) the primal Benders' decomposition method. The first method is used to coordinate TN&ADNs planning problems and the second one is implemented to solve the robust optimisation problem for TN planning. The following part describes the details of the proposed solution strategy.

3.1 Centralised model

For the sake of shortness, the compact matrix formulation, i.e. (51)–(63), is used to represent the HR&S planning of TN&ADNs, i.e. (1)–(44). The compact form of the model is

$$\min_{\{x^{\mathrm{T}}\}} \boldsymbol{I}'\boldsymbol{x}^{\mathrm{T}} + \max_{\{u^{\mathrm{T}}\}} \min_{\{y^{\mathrm{T}}, z^{\mathrm{T}}\}} \boldsymbol{C}'y^{\mathrm{T}} + \min_{\{x^{\mathrm{D}}, y^{\mathrm{D}}, z^{\mathrm{D}}\}} \left(\tilde{\boldsymbol{I}}'x^{\mathrm{D}} + \tilde{\boldsymbol{C}}'y^{\mathrm{D}}\right) \tag{51}$$

$$x^{\Omega} \in \{0, 1\}, \forall \Omega \in \{T, D\} \tag{52}$$

$$Tx^{\Omega} \le W, \quad \forall \Omega \in \{T, D\} \tag{53}$$

$$\boldsymbol{I}'x^{\Omega} \le \Theta^{\Omega}, \quad \forall \Omega \in \{T, D\} \tag{54}$$

$$Ay^{\Omega} \le Bx^{\Omega} : \kappa_1^{\mathrm{T}}, \quad \forall \Omega \in \{T, D\} \tag{55}$$

$$Dy^{\Omega} = E : \kappa_2^{\mathrm{T}}, \quad \forall \Omega \in \{T, D\} \tag{56}$$

$$Fy^{\Omega} + Gx^{\Omega} \le H : \kappa_3^{\mathrm{T}}, \quad \forall \Omega \in \{T, D\} \tag{57}$$

$$Jy^{\Omega} \le K : \kappa_4^{\mathrm{T}}, \quad \forall \Omega \in \{T, D\} \tag{58}$$

$$Ly^{\Omega} + Vz^{\Omega} = Mu^{\mathrm{T}} : \kappa_5^{\mathrm{T}} \quad \forall \Omega \in \{T, D\} \tag{59}$$

$$u^{\mathrm{T}} \in U^{\mathrm{T}} \tag{60}$$

$$Ou^{\mathrm{T}} \le N : \kappa_6^{\mathrm{T}} \tag{61}$$

$$P'x^{\mathrm{D}} = Q \tag{62}$$

$$Rz^{\mathrm{T}} = Sz^{\mathrm{D}} \tag{63}$$

The objective function (51) corresponds to (1) where the superscript $(\cdot)'$ shows transpose of the vector. Note that, in (51), sets $\{\boldsymbol{x}^{\mathrm{T}}, x^{\mathrm{D}}\}$, $\{u^{\mathrm{T}}\}$, $\{y^{\mathrm{T}}\}$, and $\{y^{\mathrm{D}}\}$ represent the Ξ_1, Ξ_2, Ξ_3, and Ξ_4, respectively. Furthermore, constraints (52)–(54) mimic (3)–(8) and, in the TN model, and (24)–(29), in the ADN model, which define the investment decision variables. The superscripts $(\cdot)^{\mathrm{T}}$ and $(\cdot)^{\mathrm{D}}$ for variables in constraints (51)–(63) show the variables associated with TN and ADN models, respectively. Constraint (55) represents the inequality constraints involving binary variables, (9), (10), (15)–(17), (30), (31) and (36)–(38). Constraint (56) corresponds to (11), (12), (32), and (33), constraint (57) corresponds to (13)–(15), (34), and (36), constraint (58) represents (18), (19), (39), and (40), constraint (59) represents (20), (21), (41), and (42), constraint (60) represents the worse-case uncertainty set that corresponds to (22), constraint (61) denotes the inequality constraints involving an uncertain variable, (22). Constraint (62) mimics (43) that defines the radial configuration in the distribution network. Constraint (63) mimics (44) that expresses the coupled constraints.

3.2 Decentralised model

As mentioned, the centralised TN&ADNs planning model is not applicable because the TN and ADNs are planned individually through a TN planner and a distribution network planner. Additionally, due to the shared variable in (59) and coupled constraint (63), the TN&ADNs planning problem cannot be solved separately. Hence, a two-level hierarchical method has been proposed to decompose TN&ADNs planning problems. In brief, the two-level hierarchical method decomposes the optimal co-planning problem, i.e. (51)–(63), into two independent planning problems that the TN planning problem is located in the upper level and the ADN planning problem is in the lower level. Accordingly, the TN and each ADN planning problems are individually formulated and solved in a two-level hierarchical manner. Then, the communications and optimal coordination between the TN and ADN planning problems can be achieved with the target variable, i.e. z^{T}, in the TN planning and response variable, i.e. z^{D}, in the ADN planning. Accordingly, the TN and ADN planning problems and coordination between both planning problems can be formulated in detail as follows.

3.2.1 Upper level (robust TN planning problem): The mathematical model of TN planning can be written as follows:

$$\min_{\{x^{\mathrm{T}}\}}\max_{\{u^{\mathrm{T}}\}}\min_{\{y^{\mathrm{T}}\}}\left(\boldsymbol{I}'\boldsymbol{x}^{\mathrm{T}}+C'y^{\mathrm{T}}\right)+\alpha\left(z^{\mathrm{T}}-\hat{z}^{\mathrm{D}}\right)+\left(\beta\left(z^{\mathrm{T}}-\hat{z}^{\mathrm{D}}\right)\right)^{2} \tag{64}$$

$$\text{Constraints}(52)-(58),(60),\text{and}(61)\ \forall\Omega\in\{T\} \tag{65}$$

$$Ly^{\mathrm{T}}+V\hat{z}^{\mathrm{D}}=Mu^{\mathrm{T}}:\kappa_5^{\mathrm{T}} \tag{66}$$

Here, the objective function (64) has two terms, the first term of the objective function (64) is similar to the first term of the objective function (1), which has been described in Section 3. The second term is the penalty function related to the shared variables with the TN planner. In the second term, z^{T} and $\hat{z}^{\mathrm{D}}$ are, respectively, target and response variables between TN&ADNs planners. Therefore, TN planning is coordinated with ADN planning through these variables z^{T} and z^{D}. The penalty function consists of two terms, linear and quadratic. α and β are multipliers associated with linear and quadratic terms, respectively, and they will be updated during the iterative solution process. An important feature of the second-order penalty function is that it is a convex quadratic curve. Therefore, this quadratic penalty function can be piecewisely linearised as presented in [24].

It should be noted that in the penalty function, the target variable, i.e. z^{T}, should be determined by TN planning, while the value of the response variable, i.e. $\hat{z}^{\mathrm{D}}$, is received from the ADNs planning. Meanwhile, the TN planning constraints (65) and (66) should be satisfied. Note that $\hat{z}^{\mathrm{D}}$ in constraint (66) is a constant term determined by the ADN planning problem.

3.2.2 Lower level (stochastic ADN planning problem): The mathematical model of the ADN planning is presented by

$$\min_{\{x^{\mathrm{D}},y^{\mathrm{D}}\}}\left(\tilde{\boldsymbol{I}}'x^{\mathrm{D}}+\tilde{\boldsymbol{C}}'y^{\mathrm{D}}\right)+\alpha\left(\hat{z}^{\mathrm{T}}-z^{\mathrm{D}}\right)+\left(\beta\left(\hat{z}^{\mathrm{T}}-z^{\mathrm{D}}\right)\right)^{2} \tag{67}$$

$$\text{Constraints}(52)-(58)\text{ and }(62)\ \forall\Omega\in\{D\} \tag{68}$$

$$L\hat{z}^{\mathrm{T}}+Vz^{\mathrm{D}}=M \tag{69}$$

Similarly, the objective function (67) has two terms, the first term of the objective function (67) is related to the TC of ADN planning, i.e. (23), that has been defined in Section 3. The second term is the penalty function related to the shared variables with the ADN planner. Here, in the penalty function, the target variable, i.e. $\hat{z}^{\mathrm{T}}$, is a constant term that is determined from the TN planning problem, hence, variable z^{D} should be determined by ADN planning. Note that $\hat{z}^{\mathrm{T}}$ is a constant term in (67) and (69).

3.2.3 Convergence mechanism: The target and response variables z^{D} and z^{T} are transferred between TN and ADN planning problems, and the iterative procedure continues until the following stopping criteria are satisfied:

$$\left|z^{\mathrm{T},(v)}-z^{\mathrm{T},(v-1)}\right|\le\varepsilon \tag{70}$$

$$\left|z^{\mathrm{D},(v)}-z^{\mathrm{D},(v-1)}\right|\le\varepsilon \tag{71}$$

$$\left|z^{\mathrm{T}}-z^{\mathrm{D}}\right|\le\varepsilon \tag{72}$$

where ε is the pre-specified error level; the superscript (v) marks the vth circulated iterative calculation between TN&ADNs planning problems; $|*|$ is the absolute value of $*$.

3.3 Decomposition algorithm

The min–max–min problem of (64)–(66) cannot be solved directly via the commercial standard optimisation packages. Accordingly, a primal Benders' decomposition method is introduced which decomposes the original problem into a master problem and a sub-problem under uncertainty. The detailed formulations for the master problem and sub-problem, plus the detailed solution method steps are described below.

3.3.1 Master problem: The master problem of the primal Benders' decomposition method, including primal cutting planes, finds the optimal values of the vectors $\boldsymbol{x}^{\mathrm{T}}$, z^{T} and $\boldsymbol{\theta}$. The formulation of the master problem can be written as follows:

$$\min_{\{x^{\mathrm{T}}\}}\boldsymbol{I}'\boldsymbol{x}^{\mathrm{T}}+\boldsymbol{\theta}+\alpha\left(z^{\mathrm{T},(v)}-\hat{z}^{\mathrm{D}}\right)+\left(\beta\left(z^{\mathrm{T},(v)}-\hat{z}^{\mathrm{D}}\right)\right)^{2} \tag{73}$$

$$(52)-(58)\text{ and }(61)\ \forall\Omega\in\{D\},u=\hat{u}^{\mathrm{T}} \tag{74}$$

$$\boldsymbol{\theta}\ge C'y^{\mathrm{T},(v)} \tag{75}$$

$$Ly^{\mathrm{T},(v)}+V\hat{z}^{\mathrm{D}}=M\hat{u}^{\mathrm{T}} \tag{76}$$

Constraints (74)–(76) denote the primal cuts. Note that index v denotes the iteration counter.

3.3.2 Sub-problem: The sub-problem finds the optimal value of the worst-case realisation of $\hat{u}^{\mathrm{T}}$. The max–min sub-problem considering the uncertainty pertaining to WEG can be written as follows:

$$\max_{\{u^{\mathrm{T}}\}}\min_{\{y^{\mathrm{T}}\}}\left(C'y^{\mathrm{T}}\right) \tag{77}$$

$$\text{Constraints}(52)-(58),(60),\text{and}(61)\ \forall\Omega\in\{T\} \tag{78}$$

$$Ly^{\mathrm{T}}+V\hat{z}^{\mathrm{D}}=Mu^{\mathrm{T}}:\kappa_5^{\mathrm{T}} \tag{79}$$

The max–min sub-problem formulation, i.e. (58)–(60), can be recast via considering the dual of the inner minimisation problem as follow:

$$\begin{aligned}\max_{\{u^{\mathrm{T}}\}}&\left(B\hat{x}^{\mathrm{T}}\right)'\kappa_1^{\mathrm{T}}+E'\kappa_2^{\mathrm{T}}+\left(H-G\hat{x}^{\mathrm{T}}\right)'\kappa_3^{\mathrm{T}}+K'\kappa_4^{\mathrm{T}}\\&+\left(Mu^{\mathrm{T}}-V\hat{z}^{\mathrm{D}}\right)'\kappa_5^{\mathrm{T}}+\left(Ou^{\mathrm{T}}\right)'\kappa_6^{\mathrm{T}}\end{aligned} \tag{80}$$

$$A'\kappa_1^{\mathrm{T}}+D'\kappa_2^{\mathrm{T}}+G'\kappa_3^{\mathrm{T}}+J'\kappa_4^{\mathrm{T}}+L'\kappa_5^{\mathrm{T}}+N'\kappa_6^{\mathrm{T}}+C=0 \tag{81}$$

$$\kappa_1^{\mathrm{T}},\kappa_3^{\mathrm{T}},\kappa_4^{\mathrm{T}},\kappa_6^{\mathrm{T}}\ge 0 \tag{82}$$

$$\kappa_2^{\mathrm{T}},\kappa_2^{\mathrm{T}},\kappa_5^{\mathrm{T}}:\text{free} \tag{83}$$

$$u^{\mathrm{T}}\in U^{\mathrm{T}} \tag{84}$$

$$Ou^{\mathrm{T}}\le N \tag{85}$$

Constraints (80)–(85) denote the constraints of the dual problem of (78) and (79). They are generated by differentiating the Lagrangian of the problems (77)–(79) with respect to operation variables y^{T}. The objective function (80) includes multiplication of $\kappa_{(\cdot)}^{\mathrm{T}}$ and u^{T}, which makes the resulting bilinear sub-problem. This problem can be solved using the approach proposed in [6].

3.4 Solution procedure

Fig. 1 illustrates the solution procedure of the proposed iterative decomposition optimisation algorithm, which determines the optimal HR&S planning results for the TN&ADNs. This algorithm has three iteration loops, loops I, II and III, which are explained as follows.

Step 0: Set the iteration index $w=0$ for loop I, $v=0$ for loop II (or sub-problem) and $k=0$ for loop III and choose initial values for $\hat{z}^{\mathrm{D}}$, $\alpha^{(k)}$, $\beta^{(k)}$, $\mathrm{UB}=+\infty$ and $\mathrm{LB}=-\infty$.

Step 2: Set $w \leftarrow w+1$. Solve the master problem (73) subject to (74)–(76) for $\hat{z}^{\mathrm{D},(w-1)}$ value obtained from the previous iteration in the loop I to obtain $z^{\mathrm{T},(w)}$.

Step 3: Solve each stochastic ADN planning problem (67) subject to (68) and (69) for $\hat{z}^{\mathrm{T},(w-1)}$ value to find $z^{\mathrm{D},(w)}$.

Step 4: Check the convergence of loop I with (70) and (71). If (70) and (71) are not satisfied, return to step 2 for the next iteration; else, go to step 5. It should be noted that in the process of the loop I of this method, α and β are fixed, and only $\hat{z}^{\mathrm{T},(w)}$ and $\hat{z}^{\mathrm{D},(w)}$ need to be updated.

Step 5: Check the convergence of loop II, i.e. (72), or stopping criteria for loop II. If it is not satisfied, go to step 6, otherwise, the converged optimal result $\hat{z}^{\mathrm{D},(w)}$ is obtained and go to step 7.

Step 6: Set $k \leftarrow k+1$ and update the values of multipliers $\alpha^{(k)}$ and $\beta^{(k)}$ using (86) and (87)

$$\alpha^{(k+1)} = \alpha^{(k)} + 2\left(\beta^{(k)}\right)^2\left(z^{\mathrm{T},(w)} - z^{\mathrm{D},(w)}\right) \tag{86}$$

$$\beta^{(k+1)} = \lambda\beta^{(k)} \tag{87}$$

where constant λ should be selected equal or larger than one in order to get the converged optimal results. This approach to updating $\alpha^{(k+1)}$ and $\beta^{(k+1)}$ is verified in [25].

Step 6: Obtain $\hat{z}^{\mathrm{D}}$, $\boldsymbol{x}^{\mathrm{T},(v)}$, and $\boldsymbol{\theta}^{(v)}$, and update the lower bound as: $\mathrm{LB} = \boldsymbol{I}'\boldsymbol{x}^{\mathrm{T},(v)} + \boldsymbol{\theta}^{(v)}$.

Step 7: Solve sub-problem (80) subject to (81)–(85) with the values of $\hat{z}^{\mathrm{D}}$ and $\hat{x}^{\mathrm{T},(v)}$ obtained from step 7 to get $\hat{u}^{\mathrm{T}}$ and update the upper bound as $\mathrm{UB} = \boldsymbol{I}'\boldsymbol{x}^{\mathrm{T},(v)} + \boldsymbol{C}'\hat{y}^{\mathrm{T},(v)}$.

Step 8: Check the convergence of loop III, i.e. $|\mathrm{UB}-\mathrm{LB}| \leq \varepsilon$; if it is satisfied to terminate the solution procedure and return the current values of $\hat{z}^{\mathrm{D}}$, $\boldsymbol{x}^{\mathrm{T},(v)}$ and $\hat{u}^{\mathrm{T}}$ as the optimal solution. Else, fix the values of $\hat{u}^{\mathrm{T}}$ to its obtained values in step 7, update the iteration counter $v \leftarrow v+1$, and return to step 2 for the next iteration for loop III.

4 Simulation results

In order to illustrate the performance of the proposed decentralised robust planning strategy for TN&ADNs, the modified IEEE 30-bus TN and IEEE 33-bus distribution network have been studied here.

Both network topologies are presented in Fig. 2. The IEEE 30-bus TN has one wind farm (WF), six GUs, 41 lines, and 20 demands. The peak load is 310 MW. One WF with 115 MW capacity has been installed at bus 11. The additional data of existing GUs, demands, and TLs are given in [26]. Also, the data of two- and four-type GUs and prospective TLs are provided in Tables 1 and 2, respectively. Two candidate GUs are allowed to install on each bus. One ADN, i.e. IEEE 33-bus distribution network, has been connected to the transmission system through bus 4. As shown in Fig. 2, the ADN consists of 33 buses, 31 distribution lines, and 32 demands. For generation and transmission planning in ADN, two-type DGs and four prospective TLs are considered whose data are described in Tables 1 and 2, respectively. The additional data of demands and feeders for the IEEE 33-bus distribution network are given in [27].

The horizon of planning is 10 years and the yearly increase rate of load consumption is 5% and WEG is 0%. As can be seen in Fig. 3, both loads and WEG have been denoted through time blocks for each year in the planning horizon [28]. As in TN, there is one WF and the scheduling period contains 10 years and each year includes five time blocks, the budget of uncertainty can adopt different integer values between 0 and $1 \times 10 \times 5 = 50$ (i.e. $0 \leq \bar{\Gamma}_w \leq 50$). The uncertainty of load demand in ADN planning over the years is modelled by a set of probable load scenarios based on the available forecasted data prior to running the proposed ADN planning problem. It should be noted that scenario generation and reduction methods are outside of the scope of this study. Another key point, the investment budgets for TN and ADN are limited to 95% of their operation costs. Finally, the simulations are carried out on a PC with an Intel Core CPU with eight processors clocking at 4.50 GHz and 16 GB RAM using GAMS 25.1 and CPLEX solver (ver. 12.6.3). In order to investigate the efficiency of the proposed planning problem and solution strategy, three case studies in the following subsections.

4.1 Comparison of de/coupled TN&ADN planning

This section compares the robust planning of coupled and decoupled TN&ADN to validate the high performance of coupled TN&ADN planning from the transmission's and distribution's perspective. Note that in the decoupled planning approach, the distribution grid in TN planning is modelled as the constant (forecasted) load connected to bus 4. Also, in this planning approach, the data exchange between TN&ADN planning is not taken into account.

Accordingly, the robust TN&ADN planning results of the decoupled/coupled planning approaches for different uncertainty budgets are given in Tables 3–7 and Figs. 4 and 5.

Important to realise that in Tables 3–7 and Figs. 4 and 5, if parameter Γ_w is fixed to zero, then the wind uncertainty in the

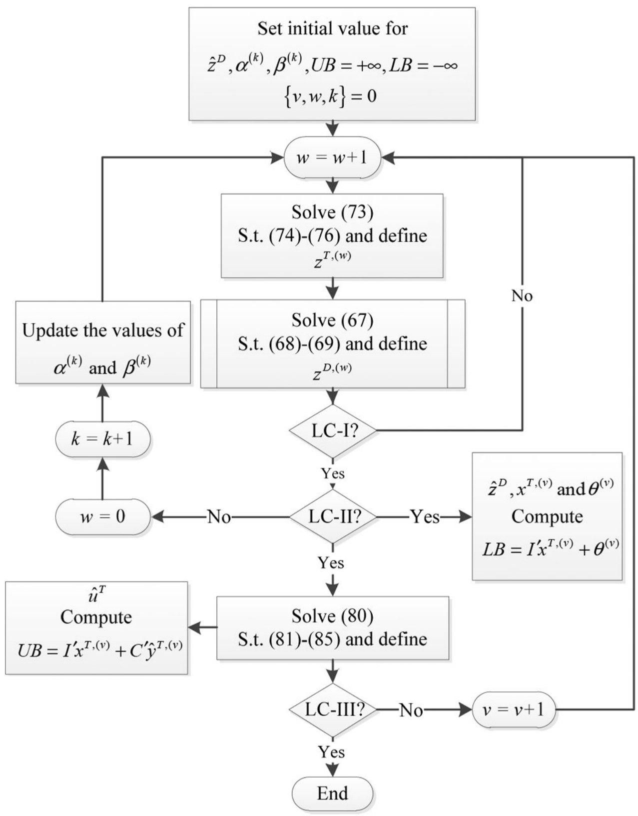

Fig. 1 *Algorithm to solve the HR&S co-planning model*

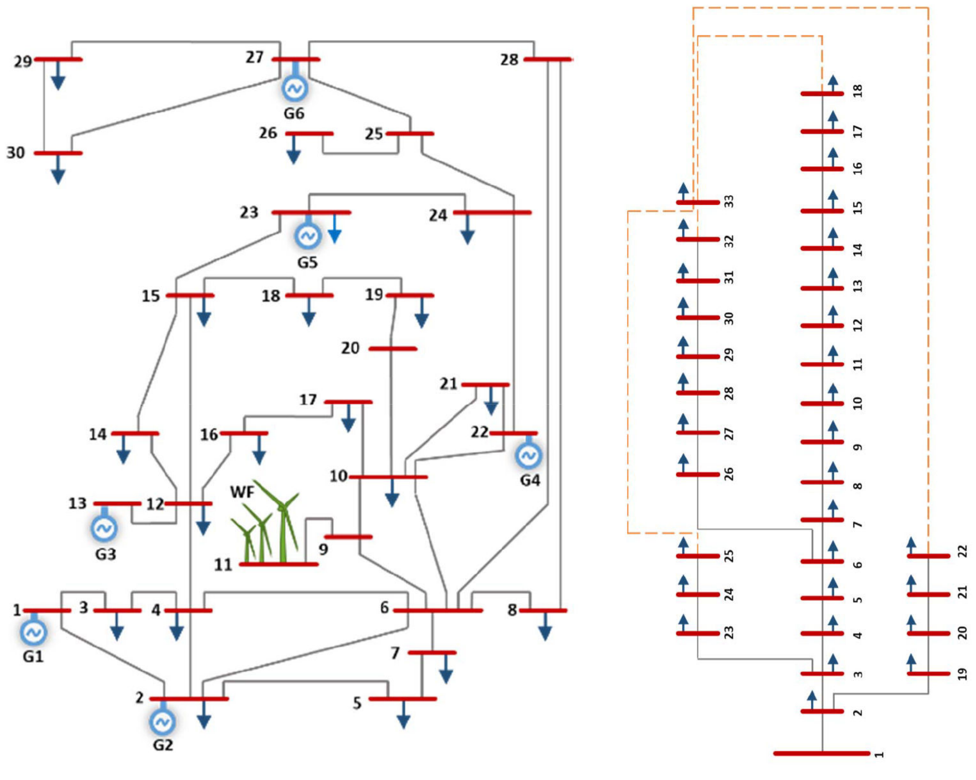

a   *b*

Fig. 2 *IEEE 30-bus test system with one ADN*
(a) 30-bus transmission test network, ***(b)*** 33-bus distribution test network

Table 1 Data of candidate TLs for TN and ADN

Network	No.	From bus	To bus	P^{max}, MW	B, p.u.	R, p.u.	IC, M$
TN	1	4	11	50	0.06	0.01	10
	2	6	11	50	0.19	0.04	15
	3	5	9	50	0.17	0.05	20
	4	26	27	50	0.17	0.05	20
ADN	1	18	33	1	0.20	0.10	2
	2	22	33	2	0.18	0.05	3
	3	25	33	2	0.12	0.02	2.1
	4	32	33	2	0.18	0.05	2.7

Table 2 GU/DG data of TN/ADN

Network	Type	P^{min}/P^{max}, MW	Q^{min}/Q^{max}, MVar	IC/OC, M$/$/MWh
TN	1	10/50	−20/20	25/30
	2	20/120	−60/60	50/20
ADN	1	0/15	−10/10	4/16
	2	0/18	−15/15	5.5/15

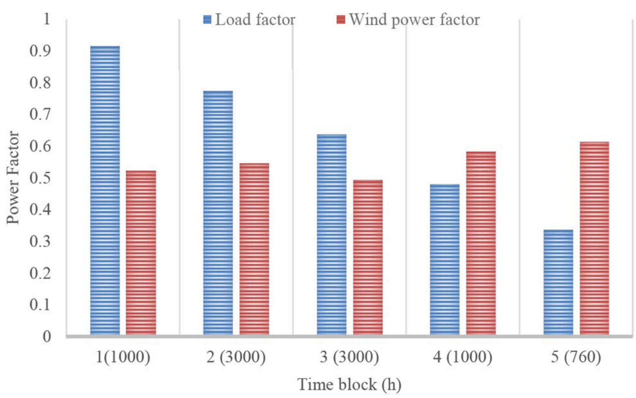

Fig. 3 *Load and wind power duration curve*

Table 3 Decoupled TN&ADNs planning results under different levels of the uncertainty budget

$\bar{\Gamma}_w$	Network	Planning	Results
0	TN	GUs	(bus 10, type 1, years 9–10)
		TLs	(line 4–11, years 1–10)
	ADN	feeders	(feeder 18–33, years 1–10)
		DGs	(bus 24, type 1, years 1–10)
50	TN	GUs	(bus 6, type 1, years 6–10)
			(bus 24, type 1, year 10)
		TLs	(line 4–11, years 1–10), (line 26–27, years 8–10)
	ADN	feeders	(feeder 18–33, years 1–10)
		DGs	(bus 14, type 1, years 1–10)

Table 4 Coupled TN&ADNs planning results under different levels of the uncertainty budget

$\bar{\Gamma}_w$	Network	Planning	Results
0	TN	GUs	—
		TLs	(line 4–11, years 1–10)
	ADN	feeders	(feeder 18–33, years 1–10)
		DGs	(bus 4, type 1, years 2–10)
		GUs	(bus 12, type 1, years 1–10)
50	TN	units	(bus 2, type 1, year 10)
		TLs	(bus 10, type 1, years 7–10)
		feeders	(line 4–11, years 1–10)
	ADN	DGs	(feeder 25–33, years 1–10)
		GUs	(bus 2, type 2, years 1–10)
			(bus 25, type 1, years 3–10)

Table 5 Decoupled TN&ADNs planning costs under different levels of the uncertainty budget

Networks	Planning costs, M$	$\bar{\Gamma}_w$		
		0	25	50
TN	IC	3.11	4.00	4.81
	OC	30.75	33.25	38.11
	TC	33.86	37.25	42.92
ADN	IC	0.60	0.60	0.60
	OC	4.55	4.55	4.55
	TC	5.15	5.15	5.15

Table 6 Coupled TN&ADNs planning costs under different levels of the uncertainty budget

Networks	Planning costs, M$	$\bar{\Gamma}_w$		
		0	25	50
TN	IC	1.50	4.00	4.81
	OC	25.24	32.74	37.87
	TC	26.74	36.74	42.68
ADN	IC	0.96	1.00	1.09
	OC	1.72	1.68	1.61
	TC	2.68	2.68	2.71

Table 7 Performance comparison of different techniques

$\bar{\Gamma}_w$	Results	Proposed decentralised technique	Centralised technique
0	TC, M$	39.37	39.42
	computation time, s	100	1356
50	TC, M$	47.41	47.50
	computation time, s	134	3215

planning decisions is not considered. However, as the value of this parameter is increased, the wind uncertainty in planning decisions is taken into account. As can be observed in Table 3, in decoupled planning approach the value of the uncertainty budget has a great impact on the TN expansion decisions including locations, and installation years of GUs and lines, while there are no changes in the ADN expansion decisions. These results were expected because in the decoupled planning approach there is no link between TN and ADN planners. However, as Table 4 illustrates, the obtained results for the coupled planning approach prove that the uncertainty budget has an impact on the ADN expansion decisions comprising locations and installation years of feeders and DGs. Besides, as can be observed in Tables 3 and 4, there are a number of important differences between decoupled and coupled planning approaches.

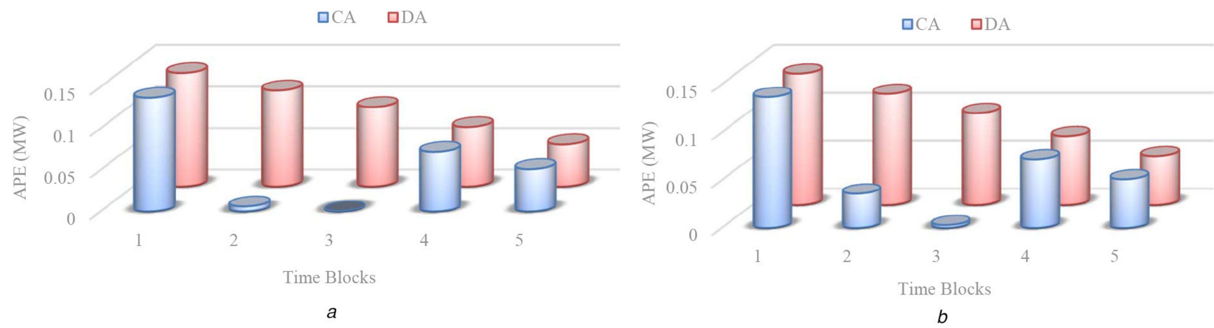

Fig. 4 *Comparison results*
(a)**, **(b) APE between TN and ADN for $\bar{\Gamma}_w = 0$ and 50, respectively

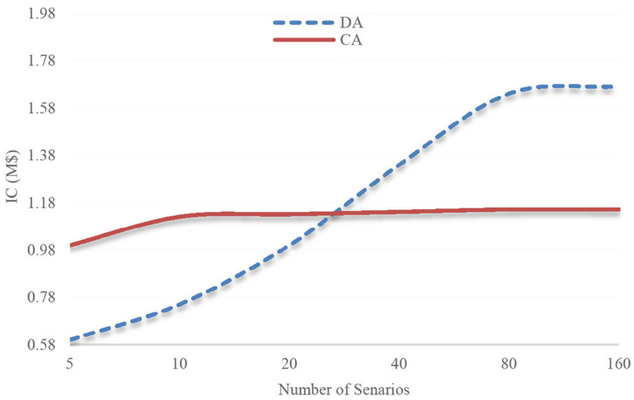

Fig. 5 *IC for ADN under different scenario number*

For instance, for $\Gamma_w = 0$, for decoupled planning approach, one GU is installed at bus 10 in TN planning, while in the coupled planning approach, building GU is not required. Similarly, as can be observed in Tables 3 and 4 for the ADN planning perspective, the feeder planning schemes for both approaches are the same, while for the coupled planning approach, more DGs are installed. However, as Tables 3 and 4 illustrate, for $\Gamma_w = 50$, the coupled planning approach can reduce line building and contribute to postponing the GUs in TLs upgrades.

The results of the planning costs for decoupled and coupled planning approaches are set out in Tables 5 and 6. The following conclusions can be drawn from Tables 5 and 6:

(i) By increasing from 0 to 50, the IC, OC, and TC increase. In fact, the main reason is that increasing the budget of uncertainty results in more conservative expansion plans for TN, which can withstand worse realisations of uncertain WEG (i.e. lower WEG). Therefore, planning costs are increased, which is indeed the price of the robustness of a more conservative expansion plan for TN.
(ii) In the decoupled planning approach for ADN, by increasing parameter Γ_w, no increase in IC, OC, and TC is detected. This result is expected. Since there is no correlation between TN and ADN planners. However, for the coupled planning approach, the budget of uncertainty can play an important role in ADN planning. Following the addition of a budget of uncertainty, an increase in the IC is recorded, while reduce in OC is detected. There are several possible explanations for this result. The reasonable explanation for this might be that with increase budget of uncertainty number of building DGs in ADN is increased (as shown in Table 4), thus, in this condition, the power generation cost in ADN is lower than power purchasing from substation or TN.
(iii) What is interesting about the data in these tables is that similar to TN planning, the OC in the coupled planning approach for ADN planning is reduced. This result was anticipated. For instance, Figs. 4*a* and *b* display the amount of active power exchanged (APE) between TN and ADN, in decoupled/coupled planning approaches, for a budget of uncertainty 0 and 50, respectively. The most interesting aspects of these figures are that in decoupled planning approach APE between TN and ADN is constant while in coupled planning approach the APE in time blocks 3 and 4 is reduced. Under this circumstance, the coupled planning approach can benefit a lot in reducing OC due to the coordination of TN and ADN.
(iv) Point often overlooked, the IC in the coupled planning approach for ADN planning increases compared with that in the decoupled planning approach. However, the IC in the coupled planning approach for TN planning decreases compared with that in the decoupled planning approach. This result was expected. However, the reason for this is probably is that in the coupled planning approach, the ADN planning scheme can play a key role in the TN planning decision. Although the IC of the ADN in the coupled planning approach increases compared with that in the decoupled planning, the OC and TC of the coupled planning approach decrease.

4.2 Impact of scenario number in ADN planning

Here, at first, set $\Gamma_w = 25$ then the number of scenarios is varied from 10 to 60, to show the impact of scenario number in decoupled and coupled planning approaches for the ADN planning perspective. The results of this impact can be found in Fig. 5. According to this figure, the number of generated scenarios for both approaches has been assigned. It can be seen from this figure that after selecting more than 10 and 80 scenarios, respectively, for the decoupled and coupled planning approaches, the value of the IC converges to a stable value. This result implies that the coupled planning approach needs a lower number of scenarios than the decoupled approach to determine the optimal IC for ADN planning.

4.3 Performance of the proposed solution strategy

Notice that in order to check the validity of the results of the proposed decentralised technique, coupled TN&ADN planning problem is also solved considering the transmission system and distribution system as a single system which is called centralised technique. Table 7 compares the results obtained from both techniques for a budget of uncertainty 0 and 50. It is apparent from this table that there were no significant differences between the proposed decentralised technique and centralised technique in terms of TC. Another key point, the analysis shows significant differences between solution times for both techniques. What is interesting about the data in this table is that by increasing the budget of uncertainty, the solution time for the centralised technique has been increased considerably while the solution times for the decentralised technique are acceptable. Accordingly, these results confirm that the proposed decentralised technique can converge to an optimal solution within an acceptable solution time for the budget of uncertainties 0 and 50.

5 Conclusions

The aim of this study was to present a decentralised hybrid robust/stochastic approach for solving the coordinated expansion planning problem of generation and transmission from the perspective of TN&ADN planners. This study has highlighted that

- The proposed robust/stochastic approach provides an effective tool to coordinate the expansion planning of transmission and distribution systems.
- Coupled TN&ADNs planning can help to postpone the upgrade, decrease the TCs for both planners, which improves the performance of the entire power system.
- The expansion planning decisions for TN&ADN highly depend on the budget of wind uncertainty. In this regard, the simulation results approve that increasing the budget of uncertainty leads to more conservative expansion plans, but with the higher generation and ICs. On the other hand, in the coupled planning approach, the IC, OC, and TC for both planners are less increased compared to the decoupled planning approach.
- From the perspective of ADN planning to converge to an optimal value in the coupled planning approach needs fewer scenarios compared with that in the decoupled planning approach.
- Compared with centralised decision making, the proposed decentralised technique has alike performance.

To consider more real situations in the problem, the proposed planning work will be extended by considering unbalanced distribution networks in our future studies. Also, modelling the uncertainties associated with other parameters such as the failure rate of the network's components could be considered as a suggestion for future work.

6 References

[1] Roldán, C., de la Nieta, A.S., García-Bertrand, R., *et al.*: 'Robust dynamic transmission and renewable generation expansion planning: walking towards sustainable systems', *Int. J. Electr. Power Energy Syst.*, 2018, **96**, pp. 52–63

[2] Hua, B., Baldick, R., Wang, J.: 'Representing operational flexibility in generation expansion planning through convex relaxation of unit commitment', *IEEE Trans. Power Syst.*, 2018, **33**, (2), pp. 2272–2281

[3] Abapour, S., Zare, K., Mohammadi-Ivatloo, B.: 'Dynamic planning of distributed generation units in active distribution network', *IET Gener. Transm. Distrib.*, 2015, **9**, (12), pp. 1455–1463

[4] Liu, J., Cheng, H., Zeng, P., *et al.*: 'Decentralized stochastic optimization based planning of integrated transmission and distribution networks with distributed generation penetration', *Appl. Energy*, 2018, **220**, pp. 800–813

[5] Silva, J., Sumaili, J., Bessa, R.J., *et al.*: 'The challenges of estimating the impact of distributed energy resources flexibility on the TSO/DSO boundary node operating points', *Comput. Oper. Res.*, 2018, **96**, pp. 294–304

[6] Dehghan, S., Amjady, N., Conejo, A.J.: 'Adaptive robust transmission expansion planning using linear decision rules', *IEEE Trans. Power Syst.*, 2017, **32**, (5), pp. 4024–4034

[7] Hadush, S.Y., Meeus, L.: 'DSO-TSO cooperation issues and solutions for distribution grid congestion management', *Energy Policy*, 2018, **120**, pp. 610–621

[8] Silva, ,J., Sumaili, J., Bessa, R.J., *et al.*: 'Estimating the active and reactive power flexibility area at the TSO-DSO interface', *IEEE Trans. Power Syst.*, 2018, **33**, (5), pp. 4741–4750

[9] Aghaei, J., Amjady, N., Baharvandi, A., *et al.*: 'Generation and transmission expansion planning: MILP-based probabilistic model', *IEEE Trans. Power Syst.*, 2014, **29**, (4), pp. 1592–1601

[10] Khorshid-Ghazani, B., Seyedi, H., Mohammadi-ivatloo, B., *et al.*: 'Reconfiguration of distribution networks considering coordination of the protective devices', *IET Gener. Transm. Distrib.*, 2017, **11**, (1), pp. 82–92

[11] Nikoobakht, A., Aghaei, J., Mardaneh, M.: 'Securing highly penetrated wind energy systems using linearized transmission switching mechanism', *Appl. Energy*, 2017, **190**, pp. 1207–1220

[12] Vahid-Pakdel, M., Nojavan, S., Mohammadi-Ivatloo, B., *et al.*: 'Stochastic optimization of energy hub operation with consideration of thermal energy market and demand response', *Energy Convers. Manage.*, 2017, **145**, pp. 117–128

[13] Alipour, M., Mohammadi-Ivatloo, B., Zare, K.: 'Stochastic risk-constrained short-term scheduling of industrial cogeneration systems in the presence of demand response programs', *Appl. Energy*, 2014, **136**, pp. 393–404

[14] Zhan, J., Liu, W., Chung, C.: 'Stochastic transmission expansion planning considering uncertain dynamic thermal rating of overhead lines', *IEEE Trans. Power Syst.*, 2019, **34**, (1), pp. 432–443

[15] Roh, J.H., Shahidehpour, M., Wu, L.: 'Market-based generation and transmission planning with uncertainties', *IEEE Trans. Power Syst.*, 2009, **24**, (3), pp. 1587–1598

[16] Alotaibi, M.A., Salama, M.M.: 'An incentive-based multistage expansion planning model for smart distribution systems', *IEEE Trans. Power Syst.*, 2018, **33**, (5), pp. 5469–5485

[17] Muñoz-Delgado, G., Contreras, J., Arroyo, J.M.: 'Multistage generation and network expansion planning in distribution systems considering uncertainty and reliability', *IEEE Trans. Power Syst.*, 2016, **31**, (5), pp. 3715–3728

[18] Amjady, N., Attarha, A., Dehghan, S., *et al.*: 'Adaptive robust expansion planning for a distribution network with DERs', *IEEE Trans. Power Syst.*, 2018, **33**, (2), pp. 1698–1715

[19] Lavorato, M., Franco, J.F., Rider, M.J., *et al.*: 'Imposing radiality constraints in distribution system optimization problems', *IEEE Trans. Power Syst.*, 2012, **27**, (1), pp. 172–180

[20] Nikoobakht, A., Aghaei, J., Niknam, T., *et al.*: 'Towards robust OPF solution strategy for the future AC/DC grids: case of VSC-HVDC-connected offshore wind farms', *IET Renew. Power Gener.*, 2018, **12**, (6), pp. 691–701

[21] Nikoobakht, A., Mardaneh, M., Aghaei, J., *et al.*: 'Flexible power system operation accommodating uncertain wind power generation using transmission topology control: an improved linearised AC SCUC model', *IET Gener. Transm. Distrib.*, 2017, **11**, (1), pp. 142–153

[22] Nikoobakht, A., Aghaei, J., Parvania, M., *et al.*: 'Contribution of FACTS devices in power systems security using MILP-based OPF', *IET Gener. Transm. Distrib.*, 2018, **12**, (15), pp. 3744–3755

[23] Pirouzi, S., Aghaei, J., Vahidinasab, V., *et al.*: 'Robust linear architecture for active/reactive power scheduling of EV integrated smart distribution networks', *Electr. Power Syst. Res.*, 2018, **155**, pp. 8–20

[24] Tosserams, S., Etman, L., Papalambros, P., *et al.*: 'An augmented Lagrangian relaxation for analytical target cascading using the alternating direction method of multipliers', *Struct. Multidiscip. Optim.*, 2006, **31**, (3), pp. 176–189

[25] Bertsekas, D.P.: '*Nonlinear programming*' (Athena Scientific, Belmont, MA, USA, 2003, 2nd edn.)

[26] motor.ece.iit.edu/data/SCUC_118

[27] Baran, M.E., Wu, F.F.: 'Network reconfiguration in distribution systems for loss reduction and load balancing', *IEEE Trans. Power Deliv.*, 1989, **4**, (2), pp. 1401–1407

[28] Zhang, X., Conejo, A.J.: 'Robust transmission expansion planning representing long-and short-term uncertainty', *IEEE Trans. Power Syst.*, 2018, **33**, (2), pp. 1329–1338